Materials Science Forum
ISSN: 1662-9752, Vol. 1184, pp 53-64
doi:10.4028/p-7lTOao

Submitted: 2026-01-16
Revised: 2026-02-16
Accepted: 2026-02-21
Online: 2026-04-14

Modeling the Effect of Lubricants on Surface Conditions in Plane-Strain Upsetting Tests

Lena Koch[1a]*, Holger Brüggemann[1b], Shakthi Bharani Tamilselvan[1c], Emad Scharifi[1d] and Junhe Lian[1e]

[1]Institute of Metal Forming (IBF), RWTH Aachen University, Germany

[a]lena.koch@ibf.rwth-aachen.de, [b]holger.bruegemann@ibf.rwth-aachen.de, [c]shakthi.tamilselvan@ibf.rwth-aachen.de, [d]emad.scharifi@ibf.rwth-aachen.de, [e]junhe.lian@ibf.rwth-aachen.de
*corresponding author

Keywords: skin-pass rolling, aluminum, roughness, FEM, coupled Eulerian-Lagrangian.

Abstract. Skin-pass rolling is commonly used to adjust the surface quality of high-strength aluminum alloys. Lubrication plays an important role in this process, as it minimizes material adhesion to the work roll, extends its service life, and also influences the contact conditions and the final surface topography. However, most numerical studies represent lubrication only through an effective friction coefficient. In this work, a finite-element framework that explicitly accounts for lubricant entrapment in engineered surface pockets by using a coupled Eulerian-Lagrangian (CEL) approach is introduced to investigate lubricant-topography interaction. The skin-pass rolling process is approximated by a plane-strain upsetting test to represent the parameters relevant for mapping the interaction between lubricant and mechanical stress, as the rolling process has a large number of influencing factors. The precipitation-hardenable aluminum alloy EN AW-6016 is modeled with rate-dependent plasticity based on experimental flow curves, while the lubricant is represented as a Eulerian material governed by an equation-of-state formulation. The effects of strain rate, friction and different lubricant filling levels in surface pockets are analyzed. The results show that variations in friction mainly affect the global force level, while the presence of lubricant leads to changes in local deformation and stress distributions. Fully filled pockets require higher forming forces due to lubricant compression, whereas partially filled pockets show behavior close to dry conditions. The CEL approach proves suitable for modeling lubricated plane-strain upsetting tests and provides a basis for further investigations of lubricated skin-pass rolling processes.

Introduction

The growing demand for lightweight design, combined with the requirement to manufacture structural components that fulfill strength specifications, has driven the development of the skin-pass rolling process for high-strength aluminum alloys in order to achieve a defined surface quality [1]. A major challenge in production is ensuring the surface quality required for subsequent coating operations [2]. To this end, a controlled surface topography is imparted to the strip by means of textured work rolls. The process is carried out under lubricated conditions to minimize material adhesion to the work roll and to extend its service life [3]. The lubricant actively participates in the forming process and affects the strip surface through hydrostatic and hydrodynamic mechanisms arising from the entrapped fluid. To develop a comprehensive understanding of the process and the underlying mechanisms, a key goal is to enable numerical simulation of lubricated skin-pass rolling. As the number of influencing variables in rolling (e.g., relative speed, temperature, friction) is substantial, a simplified analogue test is required to represent the key parameters governing the interaction between lubricant behavior and mechanical loading. A commonly used analogue test for rolling is the plane strain upsetting test, in which a sheet is compressed between two dies. This concept is proposed in the work of Kijima and Bay [4,5]. Owing to the significantly larger sheet width relative to the contact length and the sheet thickness, as well as the large roll diameter relative to the contact length, the resulting stress state approximates plane strain compression as in rolling [6]. In general,

the lubricated imprinting process consists of two primary aspects: the transfer of roughness and surface topography, and the hydrostatic and hydrodynamic behavior of the lubricant. The final surface profile emerges from the combined effect of these contributions. The reproducibility of surface roughness from the rolling process using the plane strain upsetting test has already been investigated in a previous study [7]. This work investigated whether a simplified plane-strain upsetting finite-element model can reliably approximate surface roughness transfer during skin-pass rolling. By numerically modeling die surface roughness with circular arcs and varying friction coefficients and surface pitch, the study analyzed roughness transfer mechanisms and compared the results with a macro-meso skin-pass rolling model. The work demonstrates that roughness transfer is mainly governed by die surface geometry and relative motion, while the simplified model offers much lower computational effort with comparable trends [7]. In the previous work, the lubricant was not explicitly modeled but only taken into account using the friction coefficient, whereas in the present work, fluid-structure interaction (FSI) modeling is conducted within the plane strain upsetting test on precipitation-hardenable aluminum alloy EN AW-6016. The lubricant is explicitly modeled using a coupled Euler-Lagrangian meshing approach in order to capture its influence on roughness transfer based on a simplified surface profile. It is hypothesized that conventional friction models commonly applied to lubricated forming processes, such as Coulomb or Tresca formulations, are insufficient in this context, as they fail to capture the complex interfacial mechanisms arising from the interaction between the lubricant film and the surface topography. The results are evaluated with respect to surface profiles as well as the resulting stress and strain distributions and are subsequently compared to those obtained from conventional modeling approaches.

Material and Method Modeling Framework

Coupled Euler-Lagrangian method: Simulating fluid-structure interactions is challenging, particularly when high plastic strains are present. Conventional numerical techniques frequently encounter limitations under such conditions, for example due to excessive mesh distortion or difficulties in tracking interfaces [8]. The Coupled Eulerian-Lagrangian (CEL) method provides an effective framework to overcome these issues and provide a suitable tool to model FSI. The strength of this modeling strategy is that the fluid is modeled with a Eulerian meshing approach, in which the mesh remains fixed while materials flow through it. The workpiece itself can be modeled in an Lagrangian manner, in which the mesh deforms with the material and which is mainly used in continuum mechanics applications [9]. However, large deformations will lead to severe distortion of the mesh and accordingly distortion of the individual elements. This results in numerical inaccuracies and precludes successful simulation. In a Eulerian approach, the nodes of the mesh remain fixed in space, while the material flows through elements that do not deform. Here, it is not the movement of the individual nodes that is considered, but rather the mass, momentum and energy flow through the mesh elements [10]. One disadvantage of this method is that it is difficult to track material points over time and complex geometries are difficult to represent. On the other hand, severe deformations can be represented well. This means that Eulerian elements are not always completely filled with material, some may contain only part of the material or may even be empty [11]. As a result, the boundary of the material, which usually does not align with the element boundaries, must be updated at every time step. To give the material enough freedom to move, the Eulerian mesh is usually designed as a simple rectangular grid that extends well beyond the actual material region. If the material flows outside this mesh, it is considered lost in the simulation. By combining these two representations, CEL enables the robust simulation of highly dynamic events such as fluid splashing, detonation phenomena, and object-fluid impact, without the numerical complications typically associated with mesh distortion or intricate interface-tracking procedures. An interface in Abaqus\Explicit allows information from these two approaches to be exchanged at the individual elements.

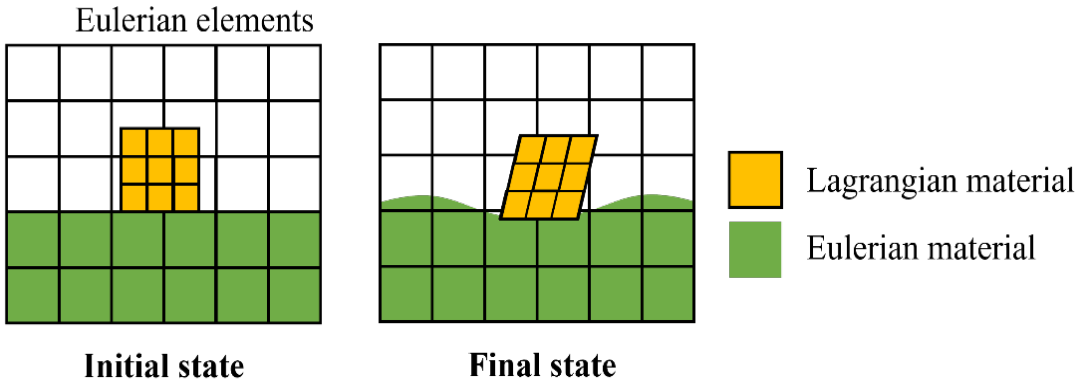

Fig. 1. Schematic representation of the Coupled Euler Lagrangian approach

The fluid dynamics are described by the Navier-Stokes equations, assuming that volume viscosity is negligible (see the corresponding (1)) [12]. Here η is the viscosity, ρ is the density, p is the pressure, v is the velocity and b represents body forces.

$$\rho\frac{Dv}{Dt} = -\nabla p + \eta\nabla^2 v + \frac{\eta}{3}\nabla(\nabla\cdot v) + \rho b \tag{1}$$

The relationship between density and pressure is defined through a so-called Equation of State (EOS). The pressure in the lubricant is determined using a linear Us–Up Hugoniot formulation of the Mie–Grüneisen EOS [13]. With this approach, the lubricant is treated as a compressible viscous fluid. This results in the following equation.

$$p = \frac{\rho_0 c_0^2 \eta}{(1-s\eta)^2}\left(1-\frac{\Gamma_0\eta}{2}\right) + \Gamma_0\rho_0 E_m \tag{2}$$

Here, is p the pressure, ρ_0 the reference density, E_m is the specific energy, Γ_0 is the Grüneisen ratio. Furthermore $c_0$and s are defined by a linear relation between the shock velocity U_s and the particle velocity U_p [13].

$$U_s = c_0 + sU_p \tag{3}$$

Simulation model: A simulation model of a plane-strain upsetting test was set up in Abaqus2019\Explicit. During the process, the die moves upward and deforms the workpiece. It should be noted that, although plane strain upsetting tests show similar stress states and contact conditions, important skin-pass rolling parameters are not considered. These include the curvature of the work roll, the relative movement and velocity of the sheet, and fluid entrainment. The setup is shown in Fig. ***2***. To reduce computational time only half of the test was modeled with suitable symmetry conditions. The die is modeled as a rigid body and discretized using R3D4 elements with an element size of 1 mm. The die has a height of 5 mm, a width of 150 mm, and a depth of 10 mm. On the top of the die are three pockets in the shape of a truncated cone in a line. These have a diameter of 6 mm and a depth of 2 mm. In addition, the pockets have a center distance of 6.5 mm between each other. The pocket and resulting surface are significantly larger than those produced by skin-pass rolling, which is carried out using electric discharge texturing (EDT) on the roller. The reason for this is that the test setup should be used for validation of a numerical FSI model. In this context, it is more appropriate to start with a large pocket, especially since it is possible to produce such a pocket without EDT technology. In its initial state, the deformable workpiece has a thickness of 1.2 mm, a width of 20 mm, and a depth of 40 mm and is discretized using C3D8R elements, which are three-dimensional eight-node-brick elements with reduced integration, with an element edge length of 0.2 mm. dimensional eight-node-brick elements with reduced integration, with an element edge length of 0.2 mm. The Euler domain has the dimensions of length 20 mm, depth of 10 mm and height of 3.2 mm. It is discretized using EC3D8R elements with an approximate global size of 0.1 mm. The

lubricant is modelled with dimensions identical to the geometry of the pocket, such that the lubricant occupies the pocket without any free surface or gaps. This lubricant is assigned to the Euler domain using discrete volume fraction field. Depending on the preferred experimental requirements, the dimension of the lubricant is changed by adjusting the initial height of the lubricant relative to the depth of the pocket, such that 75% filling height corresponds to 1.5 mm filling height of the lubricant with respect to 2 mm pocket depth. The die was assigned a velocity of 30 mm/s for a total stroke of 0.12 mm. This results in a height reduction of 10 %. In the dry state a surface-to-surface contact with a coulomb friction coefficient of 0.01 to 0.28 is defined between die and workpiece.

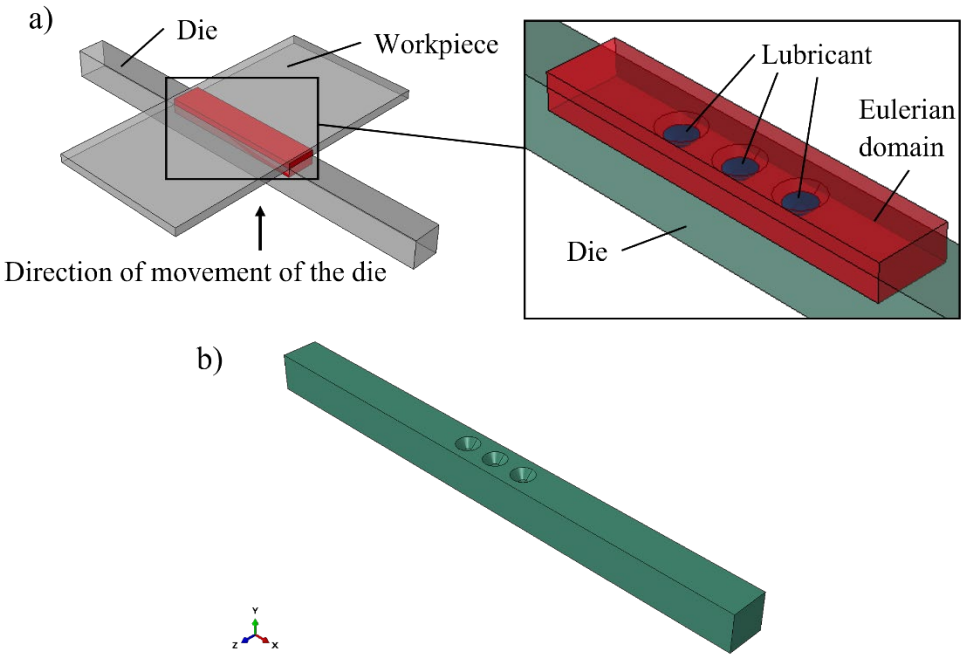

Fig. 2. a) Schematic structure of the simulation model with the Euler domain and lubricant in the initial position, here with a fill level of 50%, b) schematic structure of the die with the three pockets

Flow curves from stacked layer compression tests at room temperature and three different forming speeds were recorded (see Fig. ***3***). A pronounced strain rate dependency is observed, which was implemented in the simulation. The other material parameters such as density, Young's modulus, and Poisson's ratio of the workpiece are shown in Table 1.

Table 1. Material properties of the workpiece

Material	Density [kg/m^3]	Young's Modulus [GPa]	Poisson's ratio
EN-AW6016	2700	70	0.33

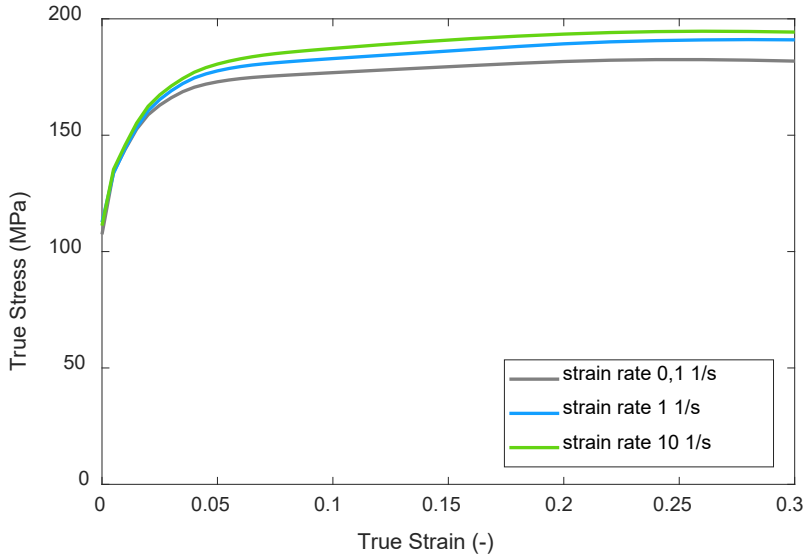

Fig. 3. Flow curves for EN AW-6016 aluminum alloy at 20 °C

The density, viscosity, sound velocity and shear modulus are required for the numerical representation of the lubricant. These values are shown in Table 2. The linear Us–Up Hugoniot form of the equation of state is used to represent the fluid properties. The contact conditions and the resulting friction behavior in the lubricated simulation with CEL are different from those in the dry state. In Abaqus, a distinction is made between the methods "General Contact" and "Surface-to-Surface Contact." "General contact" describes the hydrodynamic friction of the fluid with the workpiece with a friction coefficient of $\mu_{fluid} = 0.01$. The global "general contact" is selected here because no effective surfaces can be defined for a liquid. It ensures that the contact formulation is applied only when the Euler material with volume fraction greater than zero comes into contact with the Lagrangian surface. In addition, the "surface-to-surface contact" method with a friction coefficient of $\mu = 0.1$ is used, which locally overwrites the definition of "general contact" [14]. This contact is formulated exclusively between the rigid die and the workpiece to model the solid to solid interaction. This is restricted to Lagrangian surfaces and was not applied to Euler surface. Therefore, the force transmission can be either through the lubricant via general contact in lubricant's presence or through direct surface interactions in regions where the lubricant is not present.

Table 2. Fluid properties according to data sheet and [15,16]

Lubricant	Density [kg/m^3]	Speed of Sound [m/s]	Dynamic Viscosity [Pa·s]	Shear modulus [GPa]
Rolling oil	806.78	1333.14	0.00547	1.2

In this simulation study, the necessity of strain rate dependency is first examined, followed by an investigation of friction sensitivity. In the next step, the usefulness of the CEL method for calculating lubricated tests is demonstrated by comparing it with unlubricated tests. Finally, different filling heights of the pockets are analyzed. Consequently, this work consists of four different investigations (see **Table 3.**). The investigation of the effect of the coefficient of friction μ without explicit consideration of the lubricant using CEL serves to analyze the general sensitivity of the test setup to the friction conditions. Without such a study, a potential effect of the lubricant cannot be considered in isolation.

Table 4. Overview of the individual investigations, including the respective simulation boundary conditions

Number		Meshing approach	Friction
Investigation of strain rate dependence			
1	With strain rate-dependent material data	Lagrangian	μ = 0.1
	Without strain rate-dependent material data	Lagrangian	μ = 0.1
Friction sensitivity			
2	Conventional friction-based simulations	Lagrangian	μ = 0.01, 0.1 and 0.28
Comparison of lubricated and unlubricated simulation			
3	Unlubricated	Lagrangian	μ = 0.1
	Lubricated	CEL	"surface to surface contact" method with a friction coefficient of μ = 0.1
Investigation at different filling levels			
4	75 % filling level 95 % filling level 100 % filling level	CEL	"surface to surface contact" method with a friction coefficient of μ = 0.1

Results

Investigation of strain rate dependence: First, the force-displacement curves from a simulation with strain rate dependence and a simulation without strain rate dependence were compared in the unlubricated state as shown in Fig.4. In both simulations, the Coulomb friction coefficient is μ = 0.1. It can be observed that in the case of strain rate dependency a 2 kN higher force is present. This is due to the fact that, as can be seen in Fig. ***3***, the stress increases at higher strain rate. As a result, all simulations are run with strain rate dependency.

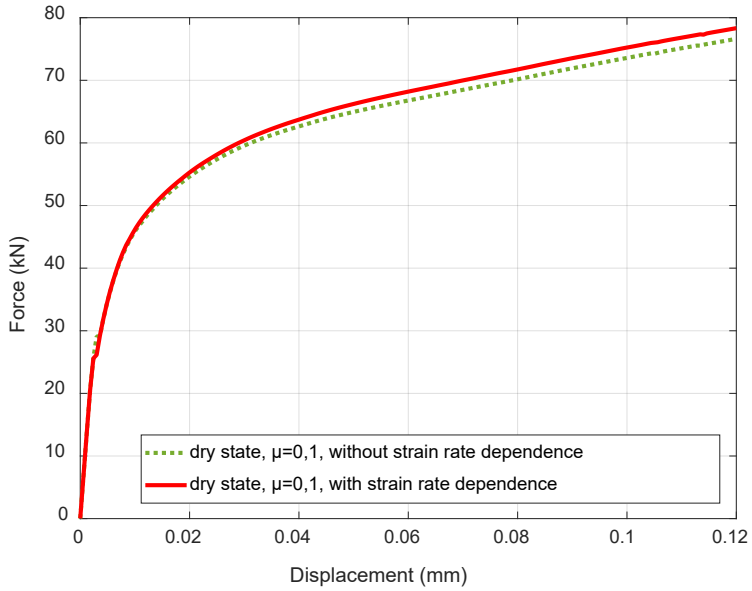

Fig.4. Force-displacement curves for the dry state simulation with and without strain rate dependence

Friction sensitivity: The next step in this work is to examine the sensitivity of the model to friction. To accomplish this, simulations were carried out with three different friction coefficients 0.01, 0.1 and 0.28. The minimum friction coefficient describes the nearly frictionless state, while the maximum

friction coefficient describes a typical value for the friction between aluminum and steel [17]. Fig. ***5*** a) shows that the force required for forming increases as the friction coefficient increases. Observing the progression of the Y coordinate at different friction coefficients at the last time increment, it is noticeable that the differences are not as pronounced as in Fig. ***5*** b), but are still visible. Due to symmetry, this figure only shows half of the node numbers over the Y coordinate for the last increment. The contours of the workpiece at different friction values clearly overlap, only in the transition areas from the pocket to the flat surface of the die does the simulation with a friction value of μ = 0.01 deviate slightly from the other two contours.

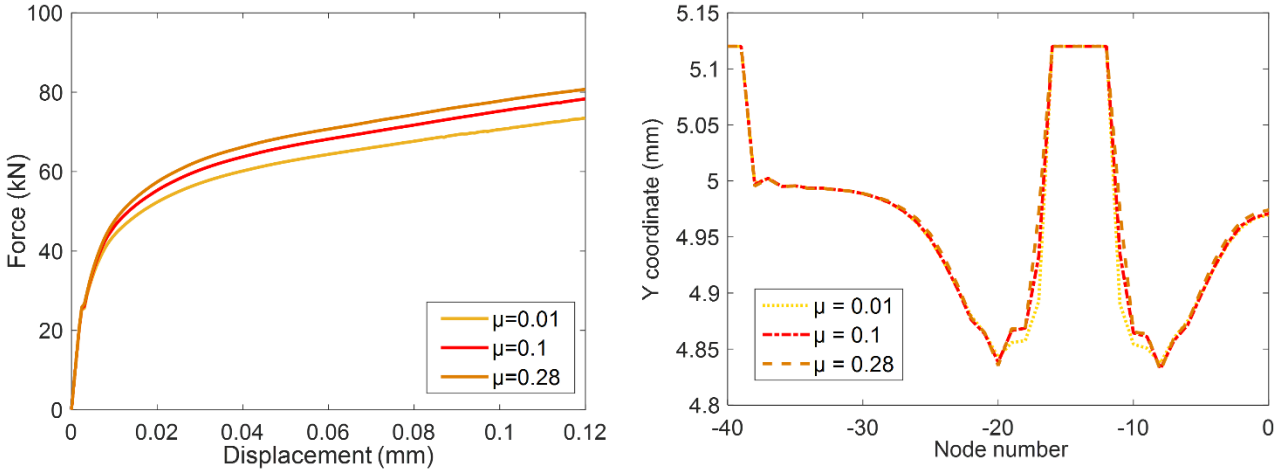

Fig. 5. a) Force against displacement for three different friction coefficients b) Point of the Y coordinate against the node number at the last time step for the three friction coefficients

Comparison of lubricated and unlubricated simulation: After examining the unlubricated condition, the CEL simulations for the lubricated condition are analyzed next. The lubricated case means that the pockets are 100% filled with lubricant. Fig. ***6*** shows the Y coordinate, the equivalent plastic strain, and the von Mises stress against the X-coordinate over various time increments for the unlubricated case (solid line) and the lubricated case with CEL (dashed line). All parameters are evaluated at the same material points. The friction conditions in the unlubricated state are μ = 0.1. Here, μ = 0.1 is selected because it is an intermediate value that is closer to fully lubricated conditions. The use of μ = 0.01 was not considered appropriate because complete lubrication over the entire duration of the test is not realistic, e.g., because the lubricant can be squeezed out during the test. In addition, only the pockets are filled with lubricant at the start of the test. In general, the simulation model of the test setup does not show a high sensitivity to the coefficient of friction. In the simulation using the CEL method, a distinction is made between “general contact” and “surface-to-surface contact” as described above. Fig. ***6*** a shows that the dry and lubricated simulations do not differ from each other at time increments 1 and 5. With increasing time increments, the contours diverge from each other in the area of the pockets. This effect is particularly pronounced in the middle pocket. It can also be seen that the deformation within the pockets is less in the lubricated state than in the unlubricated state. In quantitative terms, this means that the difference in height between the lubricated and unlubricated areas in the middle pocket is approximately 0.035 mm. This is about 30% of the total height reduction of 0.12 mm. In Fig. ***6*** b, a deviation between the two simulation methods can be seen from a time increment of 20 onwards. Furthermore, it is noticeable that two peaks form on both sides in the areas between the pockets at time step 26 at a displacement of 0.12 mm. The high equivalent plastic stress at these points is due to the fact that the strain at the edge of the pockets is high because they are located deeper. Fig. ***6*** c shows the differences in the variable von Mises stress in MPa. Here, it is noticeable that the differences only become apparent in later increments. In general, the differences between the two simulation methods are smaller than for the other two variables, but they are still noticeable. It is also noticeable that the stresses differ at the edges. In this area, the differences in the last increment are up to 50 MPa.

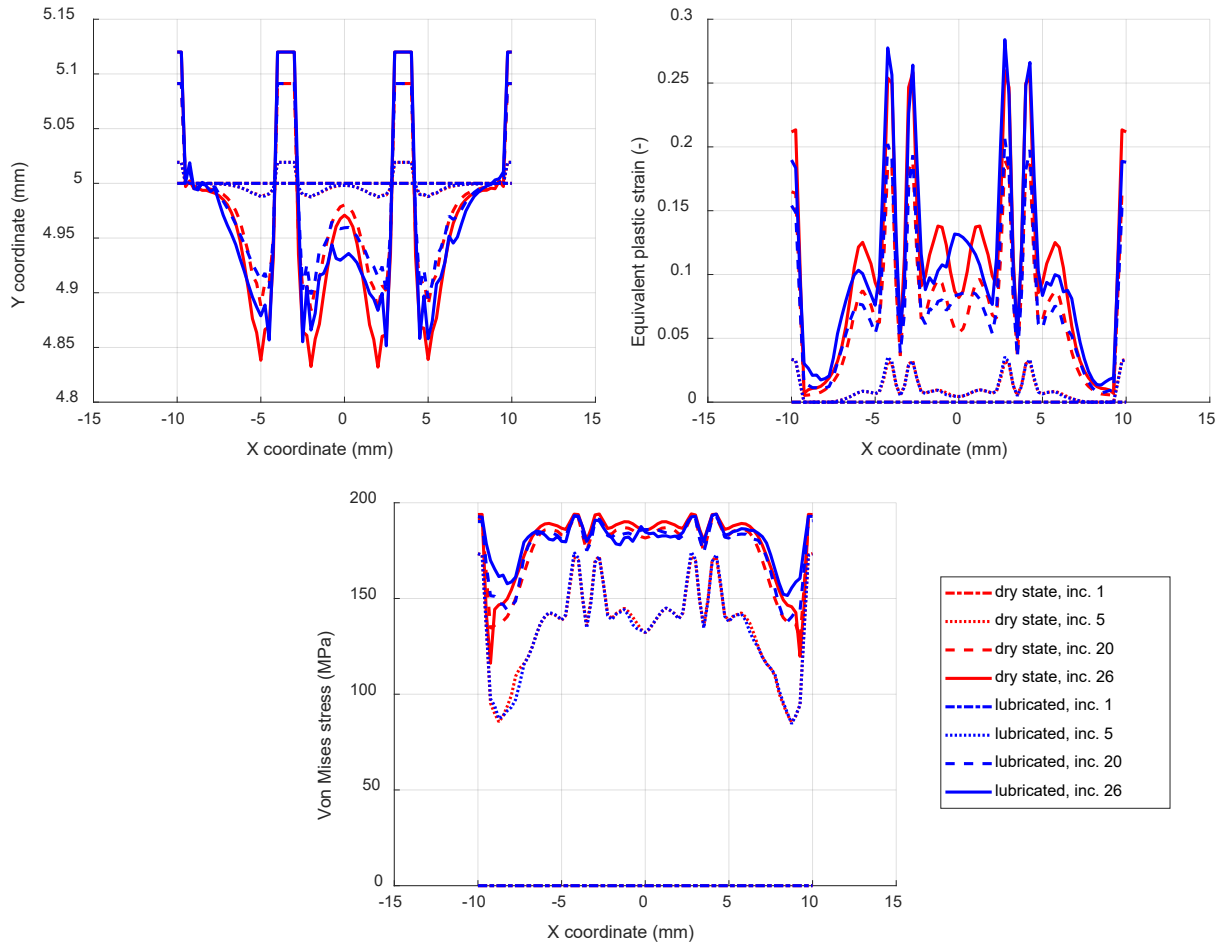

Fig. 6. Y coordinate (a), equivalent plastic strain (b), and von Mises stress (c) over the X coordinate for both dry and lubricated conditions with 100% lubricant filling

The corresponding force-displacement curves for the two simulation methods presented in Fig. ***6*** can be seen in Fig. *7*. There is a difference between the lubricated simulations with CEL and the simulations in dry conditions. The differences are over 20 kN at maximum displacement of 0,12 mm At the beginning, the two curves still lie on top of each other, but as the displacement increases, the difference between the two curves also increases, which is also caused by the different slope of both curves. Contrary to the basic assumption that the force is lower in lubricated tests than in the same unlubricated test, this study shows the opposite to the result. According to DIN 50323 Part 3, friction is defined as an interaction between contacting material areas of bodies that counteracts relative motion, whereby interface interactions between solids, liquids, and gases can occur [18]. In this test setup, the relative movement is relatively small, with a height reduction of 10% of the workpiece, so that the influence of friction is generally relatively small. Since the pocket is completely filled with lubricant in the lubricated simulation, additional force must be applied to compress the lubricant in the pocket or to push it out of the pocket at very high height reductions.

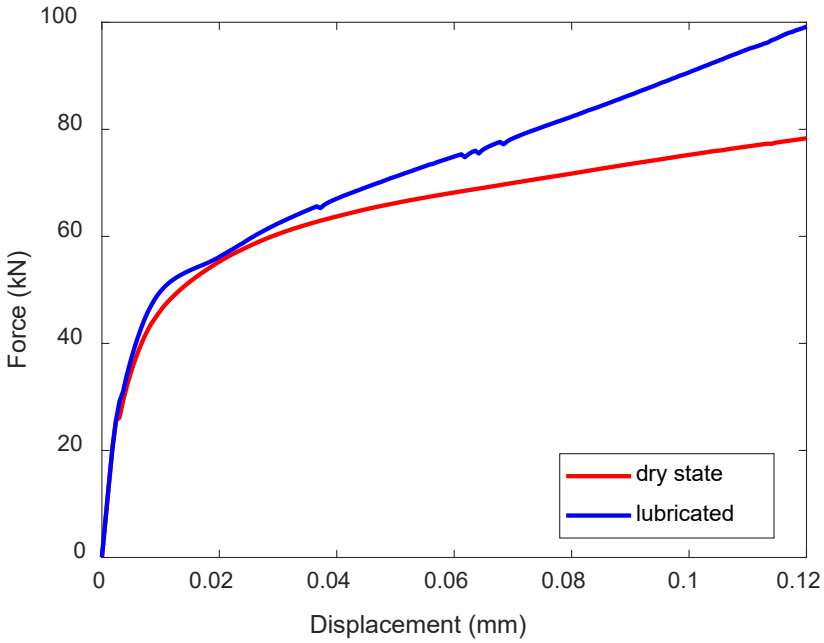

Fig. 7. Force displacement curve for the lubricated and dry state

Investigation at different filling levels: In a further simulation study, the influence of the amount of lubricant within the pocket was investigated. For this purpose, in addition to the unlubricated simulation and the simulation with 100% filling, a simulation with 75% and one with 95% pocket filling were also calculated. In the case of 75% filling, the height reduction is not sufficient for the lubricant in the pocket to come into contact with the workpiece. As a result, the force-displacement curve is almost identical to the unlubricated curve (see Fig. ***8***). In the case of 95% pocket filling, there is no contact between the workpiece and the fluid at the beginning. However, during the forming process, the lubricant comes into contact with the die. This behavior can also be seen in the force-displacement curves, as the curve with complete filling lies slightly above this.

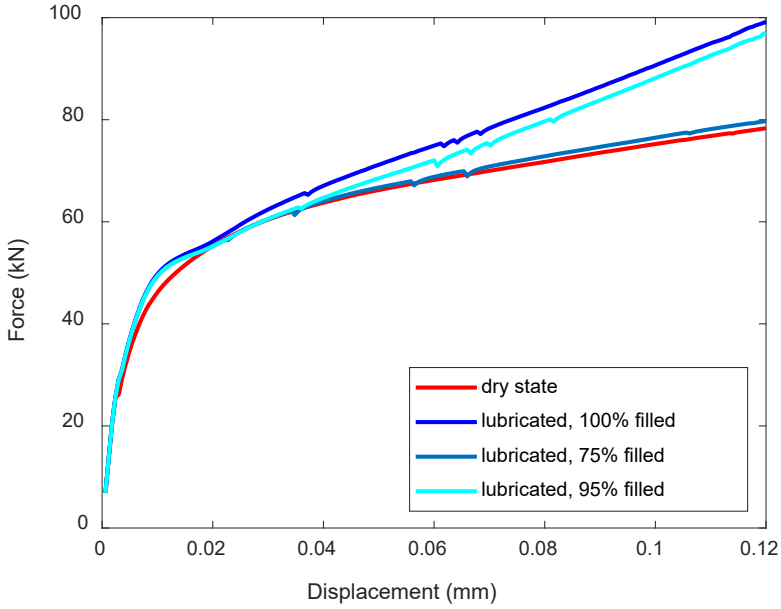

Fig. 8. Force displacement data at different filling level

Fig. 9 shows the variables Y coordinate, equivalent plastic strain, and von Mises stress against the X coordinate for the three different fill levels. At a fill level of 75%, the strain is higher in the area of the pockets. This is also reflected in Fig. ***9*** a in the course of the X and Y coordinates.

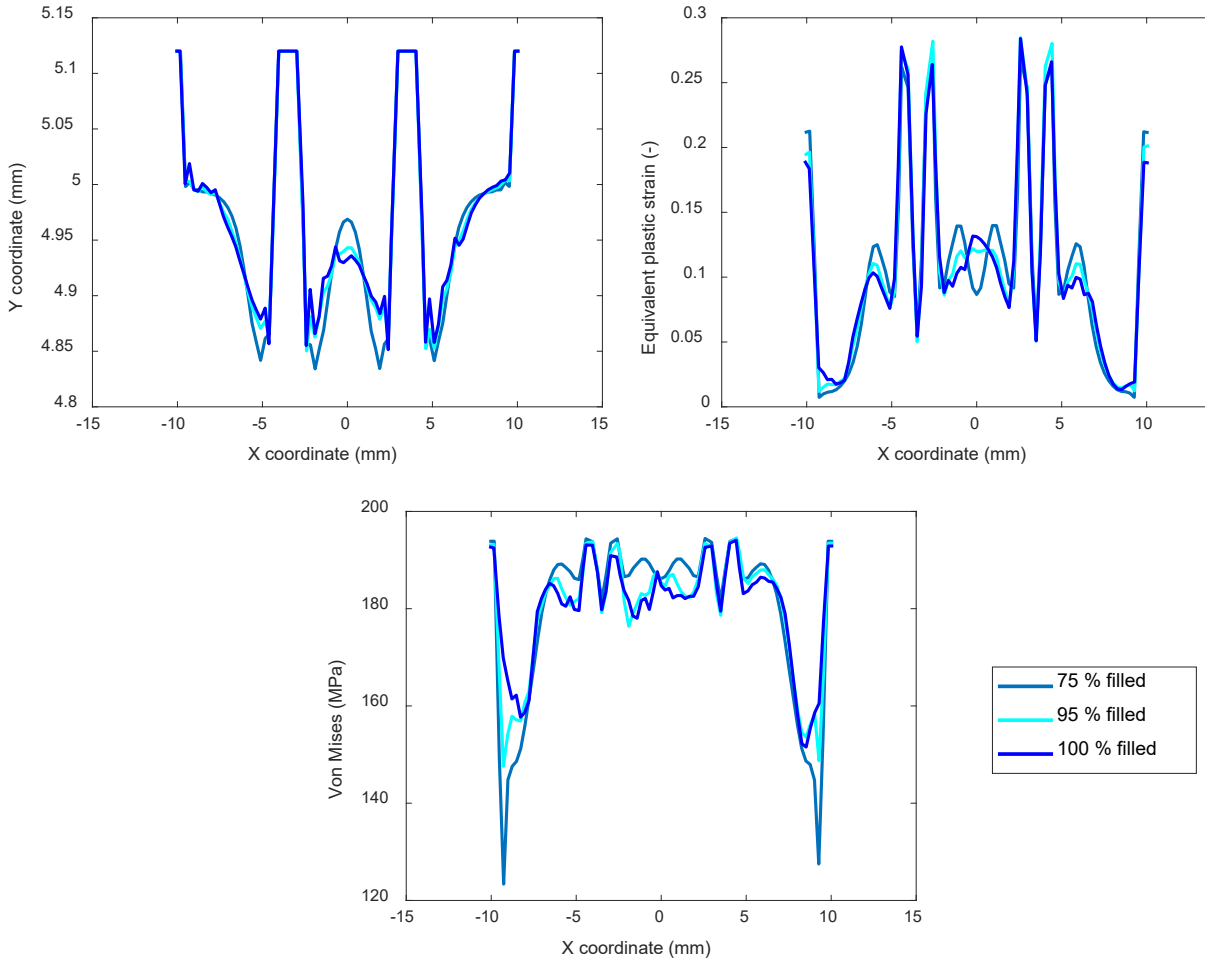

Fig. 9. Y coordinate (a), equivalent plastic strain (b), and von Mises stress (c) over the X coordinate for three different filling level

Discussion

The obtained results in the present study indicate that, while conventional friction-based models adequately capture the global forming behavior under unlubricated conditions, they fail to provide an accurate description once lubricant accumulation within surface pockets modifies the interfacial mechanics. The initial comparison between simulations with and without strain rate dependency highlights the necessity of incorporating rate-dependent material behavior for EN AW-6016. Without taking different forming speeds into account, neglecting strain rate effects leads to a underestimation of the forming force in the total amount of 2500 N. This confirms that accurate flow curve representation is essential for quantitative predictions and should be considered within these analogue models. The friction sensitivity study shows that increasing the Coulomb friction coefficient leads to higher forming forces. However, the influence of friction on the overall deformation profile and material flow is comparatively small, particularly away from the pocket transition regions. This is likely due to the fact that normal compression dominates due to the comparatively large reduction in height. A detailed investigation of the individual zones in plane-strain upsetting tests, such as the sliding zone and the sticking zone, has already been carried out in a previous study [7].

This observation supports the assumption that a numerical representation of the lubricated forming process cannot be adequately described by the reduction in the coefficient of friction, as the lubricant actively participates in the forming process and thus contributes to the final surface profile. A key finding of this work is the pronounced difference between lubricated and unlubricated simulations when the pockets are filled with lubricant. Contrary to the common assumption that lubrication necessarily reduces forming forces, the CEL simulations reveal higher forces in the lubricated case

at large displacements. This behavior can be attributed to the compressibility of the lubricant within the pockets. In the CEL simulation, the contact area is larger from the outset, which means that a higher force is required for forming. As deformation progresses, additional work is required either to compress the lubricant according to the equation of state or to displace it laterally, leading to an increase in the force. This effect cannot be captured by classical Coulomb or Tresca friction models, highlighting the necessity of a CEL fluid representation when lubricant entrapment occurs. The comparison of different filling levels further emphasizes the importance of lubricant volume. At a filling level of 75 %, the lubricant does not come into contact with the workpiece, resulting in force-displacement curves and strain distributions that are nearly identical to the dry case. In contrast, at 95 % and 100 % filling, the lubricant increasingly influences the final surface profile, stress, and strain, with higher filling levels leading to increased forming forces and reduced deformation within the pockets. These results indicate the existence of a critical filling threshold above which hydrodynamic and hydrostatic effects dominate the local forming behavior. Overall, the results demonstrate that the CEL approach provides additional physical insight into lubricant-structure interactions that cannot be obtained from simplified friction models.

Summary

The present study investigates the applicability of a Coupled Eulerian–Lagrangian (CEL) approach for modeling lubricated plane-strain upsetting tests as an analogue to skin-pass rolling. The study leads to the following main conclusions:

- Strain rate dependency of the material has a measurable influence on the forming force and must be considered for realistic simulation results.
- Conventional friction models adequately describe the forming behavior without lubrication, but can reach their limits in the presence of trapped lubricants.
- Lubricant entrapment within surface pockets can lead to increased forming forces, contrary to classical expectations, due to lubricant compression and displacement effects.
- The lubricant level is a critical parameter. Below 95 % filling level, the lubricant has only a negligible effect, whereas a nearly complete filling significantly changes the force, strain, and stress distributions.

Future work will focus on systematic parameter studies of lubricant properties and the correlation of numerical results with experimentally measured surface topographies in order to further validate the model for industrial skin-pass rolling applications. For this purpose, the elastic springback will also be mapped in the simulation model, as this will enable the comparison of surface topographies. Furthermore, fluid entrapment will be analyzed in more detail in future studies. Assuming that the realistic pockets are similar in size to the surface roughness, it can be concluded that 100% entrapment is unlikely. Therefore, investigating realistic surface conditions is an important next step.

Acknowledgements

This research is funded by the Deutsche Forschungsgesellschaft (DFG, German Research Foundation, Project number 523163077) within the project “Simulative Abbildung der Fluid-Struktur-Kontakt-Interaktion in der Umformtechnik am Beispiel des Nachwalzens”.

References

[1] S. Hojda, M. Vogd, W. Kang, H. Pawelski, G. Hirt, Numerical Investigation into Aluminium Skin Pass Rolling (2016).

[2] C. Wu, L. Zhang, Surface texture transfer in skin-pass rolling under mixed lubrication, International Journal of Mechanical Sciences 286 (2025) 109858.

[3] M. Bloeck, Aluminium sheet for automotive applications, in: Advanced Materials in Automotive Engineering, Elsevier, 2012, pp. 85–108.

[4] H. Kijima, N. Bay, Modelling of skinpass rolling by elasto-plastic analysis of plane strain upsetting, Journal of Materials Processing Technology 177 (2006) 509–512.

[5] H. Kijima, N. Bay, Contact Conditions in Skin-pass Rolling, CIRP Annals 56 (2007) 301–306.

[6] H. Kijima, N. Bay, Influence of tool roughness and lubrication on contact conditions in skin-pass rolling, Journal of Materials Processing Technology 209 (2009) 4835–4841.

[7] L. Koch, Numerical mapping of the surface roughness during skin pass rolling of high strength aluminum alloys using the plane strain upsetting test, in: Material Forming: ESAFORM 2025, 2025, pp. 909–916.

[8] M.B. Liu, G.R. Liu, S. Li, Smoothed particle hydrodynamics - a meshfree method, Computational Mechanics 33 (2004) 491.

[9] K. Liu, L. Lang, W. Zhang, M. Marai, B. Liu, Coupled Eulerian–Lagrangian simulation of granular medium sheet forming process and experimental ınvestigation at elevated temperature, Int J Adv Manuf Technol 88 (2017) 2871–2882.

[10] G.T. Mase, G.E. Mase, Continuum mechanics for engineers, 2. ed., CRC Press, Boca Raton, 1999.

[11] M. Akbari, P. Asadi, Dissimilar friction stir lap welding of aluminum to brass: Modeling of material mixing using coupled Eulerian–Lagrangian method with experimental verifications, Proceedings of the Institution of Mechanical Engineers, Part L: Journal of Materials: Design and Applications 234 (2020) 1117–1128.

[12] G. Łukaszewicz, P. Kalita, Navier-stokes equations: An introduction with applications, Springer, Switzerland, 2016.

[13] M.A. Jandron, R.C. Hurd, J.L. Belden, A.F. Bower, W. Fennell, T.T. Truscott, Modeling of Hyperelastic Water-Skipping Spheres using Abaqus/Explicit.

[14] R. Lachmayer, B.-A. Behrens, T. Ehlers, P. Müller, P. Althaus, M. Oel et al., Process-Integrated Lubrication in Sheet Metal Forming, JMMP 6 (2022) 121.

[15] S. Bair, W.O. Winer, A Rheological Model for Elastohydrodynamic Contacts Based on Primary Laboratory Data, Journal of Lubrication Technology 101 (1979) 258–264.

[16] D. Will, N. Gebhardt (Eds.), Hydraulik: Grundlagen, Komponenten, Schaltungen, 4., neu bearb. Aufl., Springer, Berlin, Heidelberg, 2008.

[17] J. Slota, Ľ. Kaščák, L. Lăzărescu, Frictional characteristics of EN AW-6082 aluminium alloy sheets used in metal forming, AMME 41 (2024) 79–87.

[18] Deutsche Institut für Normung e. V., Tribology; friction; definitions, types, conditions, quantities(DIN 50323-3), 1993.

The publication of this article was funded by the RWTH Aachen University 10.13039/501100007210